THE JOURNAL OF PHYSICAL CHEMISTRY B

Article

pubs.acs.org/JPCB

# An Experimental and Computational Investigation into the Gas-Phase Acidities of Tyrosine and Phenylalanine: Three Structures for Deprotonated Tyrosine

Samantha S. Bokatzian,† Michele L. Stover, Chelsea E. Plummer, David A. Dixon,* and Carolyn J. Cassady*

Department of Chemistry, The University of Alabama, Tuscaloosa, Alabama 35487, United States

Supporting Information

**ABSTRACT:** Using mass spectrometry and correlated molecular orbital theory, three deprotonated structures were revealed for the amino acid tyrosine. The structures were distinguished experimentally by ion/molecule reactions involving proton transfer and trimethylsilyl azide. Gas-phase acidities from proton transfer reactions and from G3(MP2) calculations generally agree well. The lowest energy structure, which was only observed experimentally using electrospray ionization from aprotic solvents, is deprotonated at the carboxylic acid group and is predicted to be highly folded. A second unfolded carboxylate structure is several kcal/mol higher in energy and primarily forms from protic solvents. Protic solvents also yield a structure deprotonated at the phenolic side chain, which experiments find to be intermediate in energy to the two carboxylate forms. G3(MP2) calculations indicate that the three structures differ in energy by only 2.5 kcal/mol, yet they are readily distinguished experimentally. Structural abundance ratios are dependent upon experimental conditions, including the solvent and accumulation time of ions in a hexapole. Under some conditions, carboxylate ions may convert to phenolate ions. For phenylalanine, which lacks a phenolic group, only one deprotonated structure was observed experimentally when electrosprayed from protic solvent. This agrees with G3(MP2) calculations that find the folded and unfolded carboxylate forms to differ by 0.3 kcal/mol.

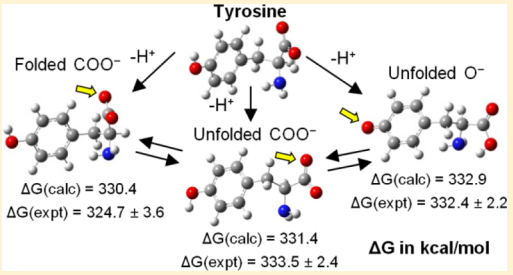


## INTRODUCTION

The amino acids tyrosine and phenylalanine often have similar properties because both possess aromatic, hydrophobic side chains. Their structures (shown in Chart 1) are similar with tyrosine having a 4-hydroxybenzyl group at the side chain and phenylalanine having a benzyl side chain. Tyrosine possesses two acidic functionalities capable of deprotonation, the carboxylic acid group and the phenolic hydroxyl group. In the gas phase, most amino acids and peptides deprotonate at the C-terminal carboxylic acid group (if such a group is present). Exceptions include aspartic acid and glutamic acid, which have carboxylic acid groups located on the side chain and can deprotonate readily on either the C-terminus or the side chain.[1] Another exception is cysteine, which has been shown to deprotonate on the side chain,[2−4] with theory[3] and experiment[4] indicating that a proton is shared between the deprotonated sulfur at the side chain and the deprotonated C-terminal carboxylate group. An infrared spectroscopy study suggested that the carboxylic acid group was deprotonated in cysteine, but this still can allow for the shared hydrogen between the two anionic sites.[5] In the context of a peptide backbone, the carboxylic acid functionality becomes part of the amide linkage except at the C-terminus, thus removing a likely deprotonation site. However, deprotonation of peptides lacking highly acidic sites has been observed experimentally.[6,7] Thus, alternative deprotonation sites are accessible using common mass spectrometry ionization techniques such as electrospray ionization (ESI).

Kass and co-workers have studied deprotonated tyrosine experimentally and theoretically, with a focus on determining if the deprotonated ion has a carboxylate or phenoxide structure.[8,9] These researchers developed a useful ion/molecule reaction involving trimethylsilyl azide ($TMSN_3$) to distinguish between carboxylate and phenoxide ions.[8,9] They employed this chemical probe to study the effects of the solvent system on deprotonated tyrosine structures produced by ESI and found that phenoxide is favored when the solvent includes methanol, while carboxylate dominates when acetonitrile or acetonitrile/

**Chart 1**

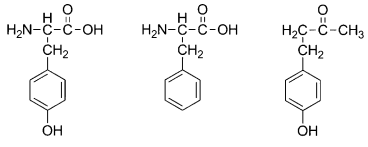


**Received:** October 3, 2014
**Published:** October 9, 2014




dx.doi.org/10.1021/jp510037c | J. Phys. Chem. B 2014, 118, 12630−12643

water solvents are used.[8] Disparate results from photoelectron spectroscopy (PES) experiments indicate that the carboxylate ion is dominant.[9] Kass and co-workers attributed this inconsistency between their $TMSN_3$ and PES experiments to different ESI source configurations. The PES experiments, which found carboxylate ions, used a home-built ESI source in which ions leaving the skimmer region pass through an ion guide for 100 ms. The ion/molecule reactions with $TMSN_3$, which found primarily phenoxide ions, employed a commercial ESI source where ions leaving the skimmer are accumulated in a hexapole trap for 1−5 s prior to their introduction into the mass analyzer. Using density functional theory (DFT) calculations (B3LYP/aug-cc-pVDZ), Kass and co-workers found a carboxylate structure to be energetically favored by 0.2 kcal/mol over a phenoxide structure.[9] This very small difference would suggest the existence of both structures in the gas phase. These researchers interpreted their results as deprotonated tyrosine undergoing a structural change as the compound goes from a solution-phase neutral to a gas-phase anion.[8]

Oomens and co-workers performed infrared multiphoton dissociation (IRMPD) on several deprotonated amino acids, including tyrosine.[5] The IRMPD spectra were compared to calculated spectra at the DFT B3LYP/6-31++G** level of theory. The amino acids were dissolved in a 80:20 (v/v) ratio of methanol ($CH_3OH$) and water ($H_2O$), which is similar to the solvent conditions where Tian and Kass[8] observed increased phenoxide production. The ESI source used by Oomens and co-workers[5] had a very similar commercial design to the source used by Kass and co-workers[9] for the $TMSN_3$ reactions; both sources employed hexapole accumulation times of several seconds. However, the experimental IRMPD results show that deprotonated tyrosine is a carboxylate in the gas phase, with no evidence of phenoxide. We previously predicted[3] that tyrosine is deprotonated at the C-terminal carboxylate site using a variety of correlated molecular orbital (MO) theory methods up through CCSD(T)/aug-cc-pVTZ.[10,11] Our higher level calculations show that the carboxylate ion is more stable than the phenoxide ion by ∼2 kcal/mol, which is consistent with the IRMPD experimental results. Using lower level DFT, Li et al.[12] have found that the experimental IRMPD spectra of Oomens and co-workers[5] are best matched to the calculated IR spectra for the carboxylate ion.

Gas-phase acidity (GA or $\Delta G_{acid}$) values are an important tool in understanding structure, reactivity, and fragmentation behavior of compounds in mass spectrometry. The GA is the Gibbs free energy change ($\Delta G$) for the reaction $AH \rightarrow A^- + H^+$. GAs or deprotonation enthalpies ($\Delta H_{acid}$) have been determined for the amino acids by O'Hair and co-workers[13] and Poutsma and co-workers[14] using the kinetic and extended kinetic methods, respectively, which involve collision-induced dissociation (CID) of a proton-bound dimer containing the analyte and a reference compound of known acidity. Poutsma and co-workers also calculated $\Delta H_{acid}$ for the common amino acids using a hybrid DFT approach with B3LYP functional combinations.[14] We have determined the GAs of glutamic acid and aspartic acid with DFT and molecular orbital (MO) computational approaches, as well as experimentally using the thermokinetic method,[15] which involves measurement of the rates of ion/molecule reactions between the deprotonated ion and reference compounds of known GA.[1] In addition, we predicted the GAs for the 20 common and 5 rare amino acids using the G3(MP2) method and obtained results consistent with experiment and with other calculations.[3] Kass and co-workers found the GA of tyrosine to be 332.5 ± 1.5 kcal/mol using equilibrium GA measurements in a dual cell Fourier transform ion cyclotron resonance mass spectrometer (FT-ICR).[9]

In our recent study of the gas-phase and aqueous acidities of the amino acids, tyrosine was studied at eight computational levels involving both DFT and MO theory.[3] In all cases, a gas-phase deprotonated carboxylate structure was predicted to be more stable on the free energy scale by 1.7−2.7 kcal/mol than a deprotonated phenoxide structure. However, as discussed above, gas-phase equilibrium proton transfer reactions and ion/molecule reactions involving $TMSN_3$ have found the phenoxide structure to be produced in the greatest abundance from protic solvents using ESI.[8,9] This difference was the motivation for the current study. Our goal was to experimentally find the lowest energy, most acidic carboxylate form of gas-phase deprotonated tyrosine.

## EXPERIMENTAL AND COMPUTATIONAL METHODS

**Mass Spectrometry.** All experiments were performed with a Bruker Daltonics (Billerica, MA, USA) BioApex 7T FT-ICR mass spectrometer. The amino acids were in the L-stereoisomer. Samples were prepared at 60 μM in solvents containing various ratios of $CH_3OH$, ultrapure $H_2O$, acetonitrile ($CH_3CN$), acetone, dimethyl sulfoxide (DMSO), tetrahydrofuran (THF), and *N*-dimethylformamide (DMF). All of the organic solvents were HPLC or LC-MS grade, except DMSO, which was ACS grade. For some solutions, 1% (by volume) of ammonium hydroxide ($NH_4OH$) was added to promote deprotonation. For experiments in which it was important to have a low water content, the solvents were also dried with 3A pore size molecular sieves.

Analyte solutions were introduced into an Apollo API source using a syringe pump set to deliver ∼90 μL/h. Electrospray ionization (ESI) employed dried air as a heated (225 °C) counter and parallel current drying gas. (The air was dried with a Labclear (Oakland, CA, USA) refillable gas filter employing RK-400 molecular sieves with a 13× pore size; the sieves also contained Drierite as a color changing indicator to denote the presence of water. The sieves were dried for at least 15 h prior to experimental use in an oven at 200 °C.) The ESI needle was grounded, while the capillary entrance and end plate were at a potential of 3.5−4.0 kV for negative ion mode analysis. Unless otherwise noted, ions produced by ESI were accumulated in a hexapole for 600−700 ms before being transported to the reaction cell by electrostatic focusing. The time used to transport ions into the cell was 10 ms.

Deprotonated ions, $[M - H]^-$, were isolated using correlated frequency ion ejection techniques.[16] Because the ions are exposed to constant pressures of neutral reactants during this isolation period, the time involved in ion isolation was kept to a minimum and was never more than 50 ms. The isolated precursor ions were then allowed to react with a reference compound introduced to the ICR cell through a leak valve at a constant pressure. Each of the ions selected for study were reacted with a series of reference compounds of known GA.[17] The reference compound pressures were measured using an ion gauge that was calibrated with the proton transfer reaction between protonated glycine and *N*,*N*-dimethylformamide, which has an experimental rate constant of 8.19 (±1.07) ×


dx.doi.org/10.1021/jp510037c | J. Phys. Chem. B 2014, 118, 12630−12643

Table 1. G3(MP2) Gas-Phase Acidities of the Carboxylic Acids and Phenols in kcal/mol

| compound | acid R group | $\Delta H_{298}$ G3(MP2) | $\Delta H_{298}$ gas expt[a] | $\Delta G_{298}$ G3(MP2) | $\Delta G_{298}$ gas expt[a] |
|---|---|---|---|---|---|
| formic acid | H | 344.7 | 345.2 ± 2.9[54] | 337.3 | 338.2 ± 2.0[54] |
| | | 344.5[b] | 345.4 ± 2.2[79] | 337.0[b] | 338.4 ± 2.0[79] |
| | | | 345.3 ± 2.2[80] | | 338.3 ± 2.0[80] |
| | | | 346.2 ± 1.2[81] | | 339.2 ± 1.5[81] |
| | | | 340.1 ± 4.6[47] | | |
| acetic acid | $CH_3$ | 348.4 | 348.6 ± 2.1[54] | 340.3 | |
| | | 348.3[b] | 348.7 ± 2.2[79] | 341.5[b] | 341.5 ± 2.0[54] |
| | | | 348.1 ± 2.2[82] | | 341.7 ± 2.0[79] |
| | | | 348.2 ± 1.4[55] | | 341.1 ± 2.0[82] |
| | | | 343.2 ± 0.7[47] | | |
| propanoic acid | $CH_2CH_3$ | 347.9 | 347.4 ± 2.9[54] | 340.0 | 340.3 ± 2.0[54] |
| | | | 347.4 ± 2.2[80] | | 340.4 ± 2.0[80] |
| isobutyric acid | $CH(CH_3)_2$ | 346.7 | 346.0 ± 2.1[80] | 338.9 | 339.0 ± 2.0[80] |
| trimethylacetic acid | $C(CH_3)_3$ | 345.3 | 345.0 ± 2.1[83] | 337.7 | 338.0 ± 2.0[83] |
| | | | 344.6 ± 2.1[80] | | 337.6 ± 2.0[80] |
| butanoic acid | $CH_2CH_2CH_3$ | 347.3 | 346.5 ± 2.2[54] | 339.4 | 339.5 ± 2.0[54] |
| | | | 346.5 ± 2.2[80] | | 339.5 ± 2.0[80] |
| | | | 346.8 ± 2.0[84] | | |
| isovaleric acid | $CH_2CH(CH_3)_2$ | 345.9 | 346.7 ± 2.1[82] | 338.5 | 339.7 ± 2.0[82] |
| | | | 345.5 ± 2.1[80] | | 338.5 ± 2.0[80] |
| *tert*-butyl-acetic acid | $CH_2C(CH_3)_3$ | 344.8 | 345.1 ± 2.1[82] | 337.4 | 338.1 ± 2.0[82] |
| | | | 344.8 ± 2.1[80] | | 337.8 ± 2.0[80] |
| pentanoic acid | $CH_2CH_2CH_2CH_3$ | 347.1 | 346.1 ± 2.4[59] | 339.1 | 339.1 ± 2.3[59] |
| | | | 346.2 ± 2.1[80] | | 339.2 ± 2.0[80] |
| isohexanoic acid | $CH_2CH_2CH(CH_3)_2$ | 346.5 | | 338.7 | |
| *tert*-butyl-propanoic acid | $CH_2CH_2C(CH_3)_3$ | 346.2 | | 337.8 | |
| phenol | | 349.5 | 348.3 ± 1.7[85] | 342.1 | |
| | | | 348.0 ± 1.0[55] | | |
| | | | 350.3 ± 2.3[54] | | 341.5 ± 1.8[85] |
| | | | 349.1 ± 2.1[86] | | 343.4 ± 2.0[54] |
| | | | 350.8 ± 0.9[87] | | 342.3 ± 2.0[86] |
| | | | 350.4 ± 3.1[88] | | 340.8 ± 1.9[89] |
| | | | 347.5 ± 1.9[89] | | |
| *o*-cresol | | 348.6 | 350.7 ± 2.9[90] | 341.4 | 342.7 ± 2.0[90] |
| | | | 349.5 ± 2.2[79] | | 342.0 ± 2.0[79] |
| *m*-cresol | | 349.9 | 350.7 ± 2.3[90] | 342.7 | 343.8 ± 2.0[90] |
| | | | 349.5 ± 2.1[79] | | 342.7 ± 2.0[79] |
| *p*-cresol | | 350.7 | 351.6 ± 2.3[90] | 342.9 | 344.7 ± 2.0[90] |
| | | | 350.2 ± 2.1[86] | | 343.4 ± 2.0[86] |
| | | | 350.2 ± 2.1[79] | | 343.4 ± 2.0[79] |

[a]The superscripted numbers provide the reference for each literature value. [b]CCSD(T) values.

$10^{-10}$ $cm^3$/molecules·s.[18] Pressures were corrected for reactant gas ionization efficiency,[19] which involved polarizabilities calculated by atomic hybrid parameter procedures.[20] Reference compound pressures were in the range $(1-10) \times 10^{-8}$ mbar. For the reactions of each precursor ion with each reference compound, at least one pressure used was from the upper half of this range and at least one pressure was from the lower half of this range; the higher and lower pressures differed by at least a factor of 4 (×4).

Reaction rate constants, $k_{exp}$, were obtained by observing the pseudo-first-order decay in reactant ion intensity as a function of trapping time. In cases where deprotonation was in competition with proton-bound dimer formation, $k_{exp}$ was obtained by fitting the experimental ion intensity data as discussed previously.[21] For experiments in which nonlinear pseudo-first-order kinetics plots (bimodal plots) indicated the presence of two ion structures reacting at two different rates, the data was fit to the sum of two exponential decays using the program Sigma Plot by Systat Software Inc. (San Jose, CA, USA). The fraction that each exponential contributes to the fit directly relates to the relative abundance of that ion structure, while the slope of each exponential decay is used to calculate the reaction rate constant (in the same manner that this information is used to calculate rate constants from a unimodal kinetics fit). This procedure has been used in the past to obtain rate constants[22−26] and gas-phase basicities[27−29] for systems containing two or three ion structures reacting at different rates.

The ratio of the experimental rate constant to the thermal capture rate constant[30,31] yields a reaction efficiency (RE). A RE of 0.269 was used as a break point, where a reaction is considered to become exoergic and a GA value is assigned. This selection of 0.269 comes from the work of Bouchoux and co-workers,[15,32−34] which has been termed the "thermokinetic method". We have found that this method provides excellent


dx.doi.org/10.1021/jp510037c | J. Phys. Chem. B 2014, 118, 12630−12643

agreement between experimental and theoretical GAs for several amino acids and small peptides.[1,6]

**Computational Methods.** The calculations were performed at the DFT and correlated MO theory levels with the program Gaussian 09.[35] The geometries were initially optimized at the DFT level with the B3LYP exchange-correlation functional[36,37] and the DZVP2 basis set.[38] Vibrational frequencies were calculated to show that the structures were minima. A range of structures were optimized to determine the most stable conformers chosen by sampling many conformations with and without hydrogen bonds. A substantial number of low energy conformers were found for the neutrals as discussed below. In our previous work on predicting the GAs of amino acids[1,3,39] and organic acids,[39] we showed that the high level G3(MP2) correlated MO method[40] gave agreement for the acidities with the experimental values to within about ±1 kcal/mol and also agreement with higher level CCSD(T) calculations extrapolated to the complete basis set limit with additional corrections.[41−45] G3(MP2) has an additional advantage over DFT methods in terms of reliable predictions for these types of compounds because the correlated MO methods in G3(MP2) perform better in the prediction of hydrogen bond energies as well as steric nonbonded interactions than do most widely used DFT exchange-correlation functionals. Thermal corrections to the enthalpies and the free energies were calculated in the scaled harmonic oscillator, rigid approximation[46] using the geometries and frequencies obtained in the G3(MP2) calculations (Hartree−Fock/6-31G* level).

**Organic Acid and Alcohol Benchmarks.** As a further benchmark of the computational methods in use, the GAs have been predicted for 11 carboxylic acids (formic, acetic, propanoic, isobutyric, trimethylacetic, butanoic, isovaleric, *tert*-butylacetic, pentanoic, isohexanoic, and *tert*-butylacetic) and 4 phenols (phenol and *ortho*-, *meta*-, and *para*-cresol). The optimized structures of the neutrals and resulting anions of the 11 carboxylic acids are shown in the Supporting Information. Conformational searches were done, and the lowest energy conformer of the neutral and anion was used for the acidity calculations. In all cases, except for isobutyric acid, the orientation of the methyl groups in the neutrals and their corresponding anions were identical. In isobutyric acid, a rotation of the two methyl groups occurred to produce the most stable anion.

Excellent agreement is found with the available experimental $\Delta H_{acid}$ and GA values of the organic acids except for the results from Muftakhov et al.[47] (Table 1). Muftakhov et al. underestimate the deprotonation enthalpies of formic and acetic acid by ∼5 kcal/mol in both cases. For formic acid, the reaction enthalpy was also calculated at a composite CCSD(T)/CBS level[41−45] to further benchmark the ability of G3(MP2) to calculate the acidities for these molecules. The components for the CCSD(T) atomization energies are given in the Supporting Information. The CCSD(T) results for formic and acetic acid[39] (Table 1) are in excellent agreement with the GAs calculated at the G3(MP2) level and the experimental values. The CCSD(T) calculations[10] were done with the augmented correlation consistent basis sets[11] and the MOLPRO[48] and NWChem[49] program systems.

The results show that the carbon chain length has only a very small effect on the acidity. Upon comparison of the acidities of butanoic and isobutyric acids, which both have four carbons in the chain, we found the additional methyl group in isobutyric acid resulted in an increased acidity of 0.5 kcal/mol. These trends follow for the other carboxylic acids as well. Carboxylic acids with two methyl groups are slightly more acidic and range from 338.5 to 338.9 kcal/mol, and those with three methyl groups are even more acidic, ranging from 337.4 to 337.8 kcal/mol.

The optimized structures for the neutrals and anions of phenol and the three cresols are given as Supporting Information. The calculated values of the phenol and cresol acidities are all within the experimental error bars, as shown in Table 1. The experimental results show that the acidity of the cresols decreases from *ortho* to *meta* to *para* with the acidity of phenol falling between *o*-cresol and *m*-cresol, giving the order *o*-cresol > phenol > *m*-cresol > *p*-cresol. The difference in acidities is only 2 kcal/mol from *o*-cresol to *p*-cresol. As the acidity difference is small, further calculations were performed to demonstrate that *p*-cresol was not lower in energy at a different computational level. The energy differences between the *ortho*, *meta*, and *para* anions were calculated at different Gx computational levels,[50−53] as shown in the Supporting Information. *o*-Cresol was predicted to be ∼1 kcal/mol more acidic than *m*-cresol with all methods except for G3B3 and G3MP2B3 where *o*-cresol was predicted to be more acidic by ∼2 kcal/mol. *o*-Cresol was predicted to be more acidic than *p*-cresol by 1.5−2 kcal/mol.

## RESULTS AND DISCUSSION

**Calculated GAs and Structures for Tyrosine, Phenylalanine, and 4-(4-Hydroxyphenyl)-2-butanone (HPB).** For deprotonated tyrosine, we have previously predicted at the G3(MP2) level that the carboxylate anion is more stable than the phenoxide by 2.5 kcal/mol.[3] The structure of the carboxylate is folded to maximize hydrogen bonding. The question exists as to whether there are additional higher energy carboxylate conformers with a similar elongated structure to that of the phenoxide. Figure 1 shows the optimized structures of the lowest energy conformer of the two amino acids and HPB and low energy conformers for the deprotonated species. Unless noted, all energies refer to free energies at 298 K. The multiple low energy conformers of the neutral amino acids are given in the Supporting Information, and in all cases, the lowest energy folded and unfolded structures differ by less than 0.5 kcal/mol. Table 2 shows the experimental and G3(MP2) calculated GAs for these molecules.

There are 22 conformers for tyrosine with energies within 2 kcal/mol of the lowest energy structure. Weak hydrogen bonding between the amine and two carbons on the phenolic ring plays an important role in the neutral, leading to a folded structure. For the tyrosine anion, we studied 10 different structures. Three low energy structures (Figure 1a) were found that differ by only 2.5 kcal/mol, two carboxylate conformers and one phenoxide isomer, in contrast to the large number of low-lying structures in the neutral. A folded structure is predicted to be the lowest energy structure for the carboxylate anion with ring C−H's interacting with the $CO_2^-$ group. The carboxylate anion has a higher energy unfolded conformer 1.0 kcal/mol less stable than the folded carboxylate conformer. The lowest energy conformer for the phenoxide anion is unfolded, is 2.5 kcal/mol less stable than the lowest energy folded carboxylate conformer, and is 1.5 kcal/mol less stable than the unfolded carboxylate conformer on the free energy scale at 298 K. In terms of $\Delta H_{298}$(gas), the energy difference between the unfolded anions is smaller, only 0.3 kcal/mol.


dx.doi.org/10.1021/jp510037c | J. Phys. Chem. B 2014, 118, 12630−12643

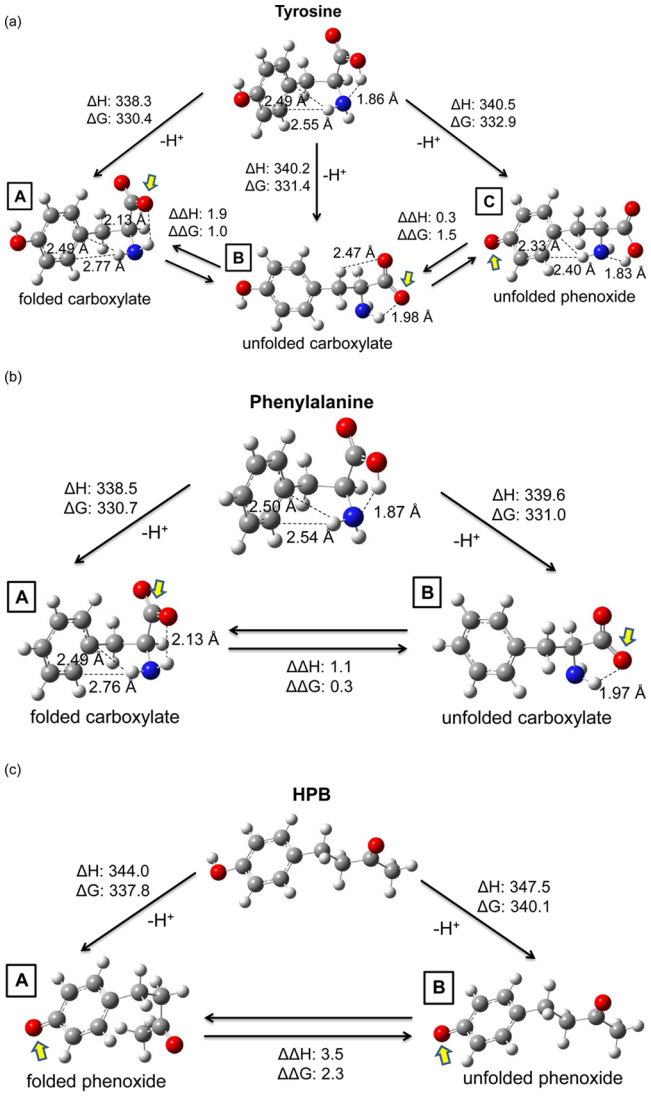


**Figure 1.** G3(MP2) results showing the structures of the most stable neutral acid and the lowest energy anions resulting from proton loss. Energies are in kcal/mol. Hydrogen bond distances are in Å. The yellow arrows show the deprotonation site. (a) Tyrosine, (b) phenylalanine, and (c) HPB.

As shown in Table 2, we have previously used a variety of Gx methods[51,52] and CCSD(T) theory to predict the energy difference between the folded carboxylate and phenoxide sites of tyrosine. We used these same methods to calculate the relative energy values for the unfolded carboxylate anion. In all cases, the folded carboxylate anion is predicted to be 1.7−2.7 kcal/mol more stable than the phenoxide and the unfolded carboxylate is between the folded carboxylate and the unfolded phenoxide. Higher energy deprotonation sites include the aromatic ring, the $\alpha$ carbon, and the amine group, and these are given in the Supporting Information for the amino acids.

Phenylalanine has 13 low energy conformers within 2 kcal/mol of the lowest energy folded structure. Deprotonation of phenylalanine (Figure 1b) forms two carboxylate structures that have G3(MP2) acidities differing by 0.3 kcal/mol with the lowest energy conformer being folded.

Neutral HPB has two low energy conformers, and the lowest energy structure is unfolded. The lowest energy phenoxide anion is folded and 2.3 kcal/mol more stable than the unfolded ion.

**Experimental GAs and Structures Produced from a Protic Solvent System.** Our experimental studies began with proton transfer ion/molecule reactions to bracket the GAs of tyrosine, phenylalanine, and HPB. This work was performed using a protic solvent mixture of 49.5:49.5:1 (v/v/v) $CH_3OH$:$H_2O$:$NH_4OH$, which is a routine ESI solvent system that often generates intense negative ions. Table 3 shows the reference compounds used in this study, their GAs, and the measured reaction efficiencies. From these results, experimental GAs were assigned. Our experimental and computational GA values are summarized in Table 2, along with literature values from other studies on these compounds.

The least acidic compound studied was HPB, which has an experimental GA of 339.6 ± 3.0 kcal/mol. (A higher GA value indicates a less acidic compound.) This agrees with our G3(MP2) calculated value of 337.8 kcal/mol, and the computational result is well within the experimental error bars. HPB was chosen for comparison to tyrosine and phenylalanine because this compound has no carboxylic acid group and, therefore, must deprotonate at its phenolic hydroxyl group.

Phenylalanine, which contains no phenolic side chain but has a carboxylic acid group at the C-terminus, is more acidic than HPB and has an experimental GA of 332.5 ± 2.2 kcal/mol, which agrees within experimental error with our G3(MP2) value of 330.7 kcal/mol. For HPB and phenylalanine, all experimental kinetics plots were linear, suggesting the presence of only one major deprotonated ion structure. If multiple structures exist, the experiments indicate that they are very similar in energy; for example, the 0.3 kcal/mol energy difference found by G3(MP2) calculations between the folded and unfolded conformers of deprotonated phenylalanine would be difficult to distinguish experimentally. There is reasonable agreement of both the calculated and experimental GAs with the experimental GA for phenylalanine of 329.6 ± 3.0 kcal/mol previously reported by O'Hair et al.[13] The fact that HPB is less acidic than phenylalanine is consistent with phenols generally being less acidic than carboxylic acids. For example, the GA of phenol is 343.4 ± 2.0 kcal/mol, while the GA of acetic acid is 341.5 ± 2.0.[54] Recently calculated GAs by Angel and Ervin[55] based on experimental enthalpies for loss of a proton are 341.5 ± 1.0 and 339.9 ± 1.7 for phenol and acetic acid, respectively, and are consistent with the above values. In both cases, the error bars overlap but the experimental results and the theoretical results in Table 1 are all consistent in the ordering between acetic acid and phenol.

Tyrosine is an interesting case because there are two potential sites of deprotonation. Using the $CH_3OH$:$H_2O$:$NH_4OH$ solvent system, two ion populations were observed in the reactions with ethyl cyanoacetate (GA = 333.6 ± 2.0 kcal/mol[17]) and 4-amino-2,3,5,6-tetrafluoropyridine (ATFP, GA = 332.8 ± 2.0 kcal/mol[17]). To illustrate this bimodal reactivity, Figure 2 gives a semilogarithmic plot of the intensity of deprotonated tyrosine, $[Tyr-H]^-$, as a function of reaction time with ethyl cyanoacetate. The experimental data (black circles) are an excellent fit to an equation involving the sum of two exponentials (black line). From the reaction efficiency data of Table 3, the less acidic deprotonated tyrosine structure accounts for ~27% of the ions and has a GA of 333.5 ± 2.4 kcal/mol, while the more acidic structure accounts for ~73% of the ions and has a GA of 332.4 ± 2.2 kcal/mol. This is


dx.doi.org/10.1021/jp510037c | J. Phys. Chem. B 2014, 118, 12630−12643

Table 2. Experimental, Theoretical, and Literature Gas-Phase Acidities in kcal/mol for Tyrosine, Phenylalanine, and HPB

| | | | | experimental | | | theoretical | |
|---|---|---|---|---|---|---|---|---|
| | experimental method | deprotonation site | conformation | $\Delta G_{298}$ gas (GA) | $\Delta H_{298}$ gas | computational method | $\Delta G_{298}$ gas | $\Delta H_{298}$ gas |
| | | | | Tyrosine | | | | |
| present work | thermokinetic | carboxylate | unfolded | 333.5 ± 2.4 | –[a] | G3(MP2) | 331.4 | 340.2 |
| | bracketing | phenolate | unfolded | 332.4 ± 2.2 | – | | 332.9[b] | 340.5[b] |
| | | carboxylate | folded | 324.7 ± 3.6 | – | | 330.4[b] | 338.3[b] |
| | | carboxylate | unfolded | | | G3B3 | 331.1 | 339.9 |
| | | phenolate | unfolded | | | | 332.6[b] | 340.3[b] |
| | | carboxylate | folded | | | | 330.5[b] | 338.3[b] |
| | | carboxylate | unfolded | | | G3 | 331.2 | 340.0 |
| | | phenolate | unfolded | | | | 332.9[b] | 340.5[b] |
| | | carboxylate | folded | | | | 330.2[b] | 338.1[b] |
| | | carboxylate | unfolded | | | G4 | 331.2 | 339.6 |
| | | phenolate | unfolded | | | | 332.3[b] | 340.1[b] |
| | | carboxylate | folded | | | | 330.6[b] | 338.3[b] |
| | | carboxylate | unfolded | | | CCSD(T)/aT//MP2/aT | 331.3 | 339.7 |
| | | phenolate | unfolded | | | | 332.3[b] | 340.1[b] |
| | | carboxylate | folded | | | | 330.6[b] | 338.2[b] |
| Kass[c] | equilibrium | carboxylate | | 332.5 ± 1.5 | 340.7 ± 1.5 | B3LYP | – | 339.5 |
| | | phenolate | | – | – | | – | 338.3 |
| | | carboxylate | | – | – | G3B3 | – | 339.9 |
| | | phenolate | | – | – | | – | 339.0 |
| Poutsma[d] | extended kinetic | – | | – | 337.7 ± 2.6 | B3LYP/6-31+G* | – | 339.2 |
| O'Hair[e] | kinetic | – | | 329.5 ± 3.0 | 336.4 ± 3.1 | – | – | – |
| | | | | Phenylalanine | | | | |
| present work | thermokinetic | carboxylate | folded | 332.5 ± 2.2 | – | G3(MP2) | 330.7 | 338.5 |
| | bracketing | carboxylate | unfolded | | | | 331.0 | 339.6 |
| Poutsma[e] | extended kinetic | carboxylate | | – | 338.9 ± 4.3 | B3LYP/6-31+G* | – | 338.7 |
| O'Hair[e] | kinetic | carboxylate | | 329.6 ± 3.0 | 336.5 ± 3.1 | – | – | – |
| | | | | 4-(4-Hydroxyphenyl)-2-butanone (HPB) | | | | |
| present work | thermokinetic | phenolate | folded | 339.6 ± 3.0 | – | G3(MP2) | 337.8 | 344.0 |
| | bracketing | phenolate | unfolded | | | | 340.1 | 347.5 |

[a]"–" indicates that no value was reported. [b]From ref 4. [c]From ref 9. [d]From ref 14. [e]From ref 13.

the first time that experimental GAs have been separately obtained for the different deprotonated tyrosine structures. Using an equilibrium method, Kass and co-workers reported a single GA value of tyrosine of 332.5 ± 1.5 kcal/mol,[9] which is in excellent agreement with our GA value relating to the more acidic structure. Using the kinetic method of CID on a proton bound dimer, O'Hair et al. obtained a value of 329.5 ± 3.0 kcal/mol,[13] which agrees to within experimental error. O'Hair's value is in excellent agreement with our calculated G3(MP2) value for the folded carboxylate.

The proton transfer reaction data clearly shows two structures for deprotonated tyrosine but does not distinguish between carboxylate and phenoxide ions. To identify these structures, we employed the ion/molecule reaction with $TMSN_3$ developed by Kass and co-workers.[8,9] Using a series of model compounds to characterize reactivity, they found that deprotonated tyrosine with the carboxylate structure reacts with $TMSN_3$ to form the azide ion, $N_3^-$ ($m/z$ 42), and a neutral tyrosine trimethylsilyl ester (TyrOTMS); in contrast, the phenoxide structure of deprotonated tyrosine silyates at the phenol group, producing $TMSOTyrCO_2^-$ ($m/z$ 252) and the neutral $HN_3$. In our work, for ion generation from a protic $CH_3OH$:$H_2O$:$NH_4OH$ solvent system, the $TMSN_3$ reaction showed that the phenoxide structure accounts for 67(±7)% of the ions, with the remaining 33(±7)% of the ions being carboxylate.

Taken together, the proton transfer and the $TMSN_3$ reactivity data indicate that the more abundant and more acidic deprotonated tyrosine species (~70% of the ions) has a phenoxide structure and yields an experimental GA of 332.4 ± 2.2 kcal/mol. This corresponds to structure C of Figure 1a, unfolded phenoxide, which has a calculated GA of 332.9 kcal/mol. The less abundant and less acidic deprotonated tyrosine species (~30%) has a carboxylate structure and an experimental of GA of 333.5 ± 2.4 kcal/mol. This corresponds to structure B of Figure 1a, unfolded carboxylate, which has a calculated GA of 331.4 kcal/mol. These structures were generated from a protic solvent system of 49.5:49.5:1 (v/v/v) $CH_3OH$:$H_2O$:$NH_4OH$. Kass and co-workers found this same phenoxide/carboxylate ratio of 70:30 when tyrosine ions were produced from a solution of 75:25 (v/v) $CH_3OH$:$H_2O$.[8,9] Thus, our results and those of Kass both show that the deprotonated phenoxide ion is the dominant gas-phase species when tyrosine is electrosprayed from a protic solvent system.

Our experiments found the GA involving the phenoxide structure to be 0.5 kcal/mol lower than the GA with the carboxylate structure. This differs from the G3(MP2) ordering, which predicts the unfolded carboxylate structure to yield a lower GA by 1.5 kcal/mol. There are several possible experimental reasons for this deviation. First, the proton transfer reactions involving the two deprotonated tyrosine reactant ion structures may have different activation barrier

**Table 3. Reaction Efficiencies for the Proton Transfer Reactions of Tyrosine, Phenylalanine, and HPB with Reference Compounds**

| | | average reaction efficiency (± standard deviation) | | | |
|---|---|---|---|---|---|
| reference compound | GA[a] (kcal/mol) | HPB[b] | tyrosine (protic solvent)[c] | tyrosine (aprotic solvent)[d] | phenylalanine |
| chloroform | 349.9 ± 2 | 0.01 ± 0.00 | –[e] | – | – |
| 4-trifluoromethyl aniline | 346.0 ± 2 | – | – | – | – |
| phenol | 342.3 ± 2 | – | – | – | – |
| acetic acid | 341.1 ± 2 | 0.07 ± 0.01<br>BREAK[f] | – | – | – |
| formic acid | 339.2 ± 2 | 0.34 ± 0.01 | – | – | – |
| isovaleric acid | 338.5 ± 2 | 0.41 ± 0.11 | – | – | – |
| trimethylacetic acid | 337.6 ± 2 | 0.41 ± 0.06 | NR[g] | NR | NR |
| *p*-chlorophenol | 336.2 ± 2 | 0.55 ± 0.04 | NR | NR | NR |
| ethyl cyanoacetate | 333.6 ± 2 | – | 0.23 ± 0.06 (24 ± 9%)[h]<br>0.03 ± 0.04 (76 ± 9%)<br>BREAK | 0.028 ± 0.019 (56 ± 7%)<br>NR (44 ± 7%) | 0.007 ± 0.001 |
| 4-amino-2,3,5,6-tetrafluoropyridine | 332.8 ± 2 | – | 0.53 ± 0.25 (30 ± 8%)<br>0.07 ± 0.01 (70 ± 8%)<br>BREAK | 0.033 ± 0.011 (61 ± 11%)<br>0.005 ± 0.004 (39 ± 11%)<br>BREAK | 0.02 ± 0.00<br>BREAK |
| 3-trifluoromethyl phenol | 332.4 ± 2 | – | 0.29 ± 0.02 | 0.29 ± 0.03 (58 ± 13%)<br>0.007 ± 0.002 (42 ± 13%) | 0.36 ± 0.02 |
| 3,3,3-trifluoropropionic acid | 326.9 ± 2 | – | 0.75 ± 0.09 | 0.38 ± 0.04 (59 ± 3%)<br>0.13 ± 0.04 (41 ± 3%)<br>BREAK | 0.79 ± 0.08 |
| difluoroacetic acid | 323.8 ± 2 | – | – | 0.45 ± 0.10 (46 ± 13%)<br>0.33 ± 0.08 (54 ± 13%) | – |
| pentafluorophenol | 320.8 ± 2 | – | – | 1.2 ± 0.27 (58 ± 15%)<br>0.51 ± 0.03 (42 ± 15%) | – |

[a]All reference compound GAs were obtained from ref 17. [b]HPB stands for 4-(4-hydroxyphenyl)-2-butanone. [c]Protic solvent system of 49.5:49.5:1 (v/v/v) $CH_3OH$:$H_2O$:$NH_4OH$. [d]Aprotic solvent system of 99:1 (v/v) $CH_3CN$:$H_2O$. [e]"–" indicates that no reaction was performed. [f]"BREAK" indicates the point where experimental GA was assigned. [g]"NR" indicates that no reaction was observed. [h]Two reaction efficiencies and the relative abundances of each are listed for reactions in which bimodal kinetics plots indicate the existence of two ion populations reacting at two different rates.

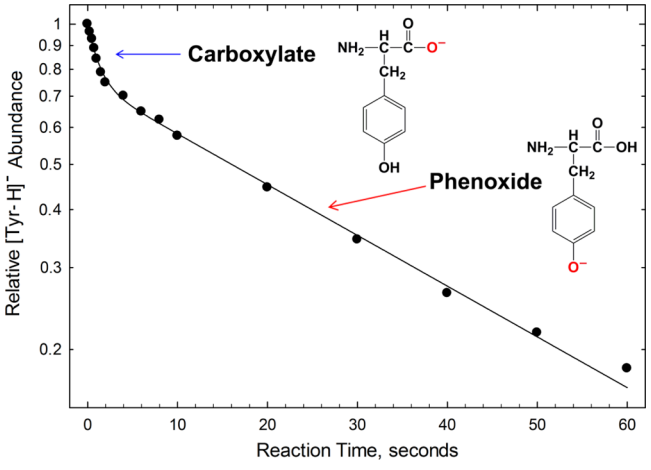


**Figure 2.** Reactant loss curve for the reaction of deprotonated tyrosine with ethyl cyanoacetate, which is present at a constant pressure of $8.9 \times 10^{-8}$ mbar. The solvent is 49.5:49.5:1 (v/v/v) $CH_3OH$:$H_2O$:$NH_4OH$. The logarithm of $[Tyr-H]^-$ intensity is plotted as a function of reaction time. The experimental data points (black circles) are fitted to an equation involving the sum of two exponential decays.

heights, which could lead to a reaction being under kinetic control as opposed to thermodynamic control. This issue is known to affect proton transfer studies of several organic molecules.[56−58] In addition, the reaction intermediate is a proton bound dimer involving deprotonated tyrosine and an acidic reference compound, $[(Tyr-H)^-\cdot H^+\cdot(A-H)^-]$. This is essentially the same type of complex that is used in the kinetic method of gas-phase basicity (GB) and GA determinations, which involves collision-induced dissociation of the dimer.[59,60] For several small organic acids, deviations from expected GAs or GBs using the kinetic method have been attributed to the dimer adapting a slightly higher energy structure in situations where double hydrogen bonding exists within the dimer or where the analyte conformation preferred in the dimer differs from that of its monomer form.[61−63] For example, Fournier et al.[62] found that the amino acid glutamic acid has bimodal dissociation plots during a GA study using the kinetic method. Using calculations at the G3(MP2) and OLYP/aug-cc-pVTZ levels, they concluded that glutamic acid could exist within the dimer in both zwitterionic and non-zwitterionic forms. Finally, steric hindrance of the reactive site, either from bulky substituents or folded conformations with hydrogen bonding, can lessen the ability of a neutral to access an ion's reactive site, which lowers the reaction efficiency and results in a lower GA assignment.[21,64,65]

As a check of the computational method, other approaches were used to predict the energy difference between the two carboxylate conformers and phenoxide isomer, as shown in Table 2. The predicted energy differences are essentially independent of the computational method. Geometries were optimized at the MP2/aug-cc-pVTZ level with diffuse functions and higher order polarization, in contrast to the G3 geometries.


dx.doi.org/10.1021/jp510037c | J. Phys. Chem. B 2014, 118, 12630−12643

Table 4. Reactions of Trimethylsilyl Azide with Deprotonated Tyrosine Electrosprayed from Various Solvents

| solvent A[a] | | solvent B[a] | | solvent C[a] | | ratios of $TMSN_3$ product ions | |
|---|---|---|---|---|---|---|---|
| name | % | name | % | name | % | % phenoxide | % carboxylate |
| $H_2O$ | 100 | | | | | 62 | 38 |
| $H_2O$ | 99 | $NH_4OH$ | 1 | | | 68 | 32 |
| $H_2O$ | 50 | $CH_3OH$ | 50 | | | 61 | 39 |
| $H_2O$ | 49.5 | $CH_3OH$ | 49.5 | $NH_4OH$ | 1 | 67 | 33 |
| $H_2O$ | 25 | $CH_3OH$ | 75 | | | 65 | 35 |
| $H_2O$ | 24.5 | $CH_3OH$ | 74.5 | $NH_4OH$ | 1 | 71 | 29 |
| $H_2O$ | 49.5 | $CH_3CN$ | 49.5 | $NH_4OH$ | 1 | 56 | 44 |
| $H_2O$ | 50 | $CH_3CN$ | 50 | | | 63 | 37 |
| $CH_3CN$ | 49.5 | $CH_3OH$ | 49.5 | $NH_4OH$ | 1 | 67 | 33 |
| $CH_3CN$ | 50 | $CH_3OH$ | 50 | | | 63 | 37 |
| $CH_3CN$ | 97 | $H_2O$ | 2 | $NH_4OH$ | 1 | 70 | 30 |
| $CH_3CN$ | 98 | $H_2O$ | 1 | $NH_4OH$ | 1 | 53 | 47 |
| $CH_3CN$ | 98 | $H_2O$ | 2 | | | 49 | 51 |
| $CH_3CN$ | 98 | $CH_3OH$ | 1 | $NH_4OH$ | 1 | 3 | 97 |
| $CH_3CN$ | 99 | $NH_4OH$ | 1 | | | 35 | 65 |
| $CH_3CN$ | 99 | $CH_3OH$ | 1 | | | 1 | 99 |
| $CH_3CN$ | 99 | $H_2O$ | 1 | | | 0 | 100 |
| $CH_3CN$ | 100 | | | | | 0 | 100 |
| acetone | 100 | | | | | 0 | 100 |
| DMF | 45 | THF | 45 | DMSO | 10 | 0 | 100 |

[a]All solvent compositions are % by volume.

Relative energies were calculated at the CCSD(T)/aug-cc-pVTZ level using optimized MP2/aug-cc-pVTZ geometries with thermal corrections, entropies, and zero point energies calculated at the MP2/aug-cc-pVDZ level. The CCSD(T) results are good to at least ±1 kcal/mol for the relative energies.

**Effects of the Solvent on Deprotonated Tyrosine: A New Carboxylate Structure.** Because the experiments with the $CH_3OH$:$H_2O$:$NH_4OH$ solvent system did not result in our finding the low energy carboxylate structure predicted by theory, additional experiments were performed. Kass and co-workers had reported that the identity of the solvent used in the ESI experiment has a dramatic effect on the phenoxide/carboxylate ratio for deprotonated tyrosine.[8,9] They found that protic solvent systems containing $CH_3OH$ favored phenoxide formation, while aprotic solvent systems containing $CH_3CN$ favored the carboxylate structure. In addition, Schröder et al.[66] found that the phenoxide/carboxylate ratio for deprotonated *p*-hydroxybenzoic acid depends on the solvent, pH, and concentration of the solution being electrosprayed.

Using the $TMSN_3$ ion/molecule reaction to distinguish between phenoxide and carboxylate ions, we electrosprayed tyrosine from a variety of solvents. These included seven solvent systems used by Tian and Kass,[8] plus 13 additional solvent systems. The results of these experiments are shown in Table 4. Exclusively (100%) carboxylate ions were found for the entirely aprotic solvents of pure $CH_3CN$, pure acetone, and a mixture of DMF, THF, and DMSO. An addition of 1% $CH_3OH$ or $H_2O$ to aprotic $CH_3CN$ has almost no effect, yielding 99−100% carboxylate ions. However, 1% addition of the base $NH_4OH$ results in 35% of the deprotonated tyrosine ions having a phenoxide structure. Addition of 2% $CH_3OH$ or $H_2O$ also has a noteworthy effect, causing about 50−70% of the ions to be phenoxide. In general, phenoxide ions appear in abundance when $NH_4OH$ or the protic solvents $CH_3OH$ or $H_2O$ are used. Our results generally agree with those of Tian and Kass,[8] although they concluded that $CH_3OH$ greatly affects the phenoxide/carboxylate ion ratio but $H_2O$ has no effect, while we found that $H_2O$ and $CH_3OH$ have a similar large effect on the ratio. For example, as our data in Table 4 indicate, ESI from a solution of 50% $CH_3CN$ and 50% of either $CH_3OH$ or $H_2O$ both result in 63% phenoxide ions and 37% carboxylate ions.

Since aprotic solvents yield almost exclusively carboxylate ions, we performed proton transfer reactions on deprotonated tyrosine produced by ESI from a solvent of 99:1 $CH_3CN$:$H_2O$. The mixture included 1% $H_2O$ solution because the presence of a trace of water greatly increased the solubility of tyrosine; however, the water content was tightly controlled and the LC-MS grade $CH_3CN$ was dried with molecular sieves to ensure that only the 1% water that we added was present. Reactions with $TMSN_3$ were performed multiple times (including in close time proximity to the proton transfer reactions) and always showed that this solvent system forms 99−100% carboxylate ions and 1 to 0% phenoxide ions.

The reaction efficiencies for proton transfer reactions of tyrosine anions produced from this aprotic solvent are given in Table 3. For all six reference compounds, two deprotonated tyrosine ion populations reacting at different rates were observed. To illustrate this, Figure 3 shows the semilogarithmic plot of the intensity of $[Tyr-H]^-$ as a function of reaction time with the reference compound was ATFP. The plot indicates that ∼71% of the ions are reacting with ATFP (albeit slowly), while the remaining ions are almost nonreactive. Using the data of Table 3, the faster reacting (less acidic) species was found to account for 61(±11)% of the ions and to involve a GA of 333.5 ± 2.4 kcal/mol. The slower reacting (more acidic) species includes 39(±11)% of the ions and yields a GA of 324.7 ± 3.6 kcal/mol. Because there is ∼9 kcal/mol difference in acidities, these two species are readily distinguished by ion/molecule reactions.

This most acidic structure for deprotonated tyrosine, yielding an experimental GA of 324.7 ± 3.6 kcal/mol, was not produced from the protic solvent system. This ion only forms in aprotic solvent, and the $TMSN_3$ reactions indicate that it has a


dx.doi.org/10.1021/jp510037c | J. Phys. Chem. B 2014, 118, 12630−12643

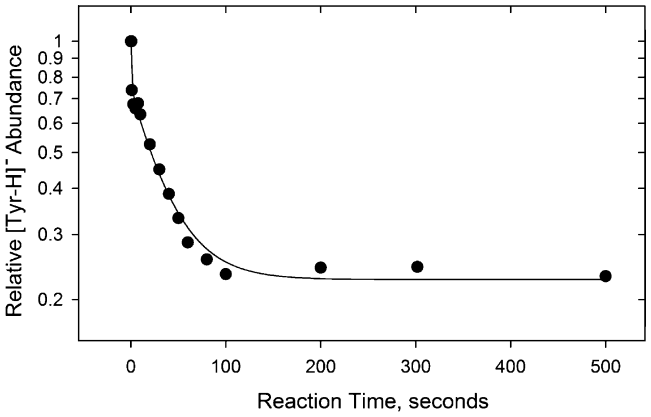


**Figure 3.** Reactant loss curve for the reaction of deprotonated tyrosine with 4-amino-2,3,5,6-tetrafluoropyridine (ATFP), which is present at a constant pressure of $5.6 \times 10^{-8}$ mbar. The solvent is 99:1 (v/v) $CH_3CN$:$H_2O$. The logarithm of $[Tyr-H]^-$ intensity is plotted as a function of reaction time. The experimental data points (black circles) are fitted to an equation involving the sum of two exponential decays.

carboxylate structure. Therefore, this is the lowest energy deprotonated tyrosine with a carboxylate structure that our calculations had previously predicted. The G3(MP2) calculated GA involving the folded carboxylate, structure A of Figure 1a, is 330.4 kcal/mol. This value is 5.7 kcal/mol higher than the experimental GA, which is a greater deviation than we typically find between experiment and theory. However, the calculations indicate that this structure is highly folded with the deprotonated carboxylate group participating in two hydrogen bonds. Due to its highly folded structure, the experimental GA value relating to this structure is likely to have more error than the other experimental GA values obtained this study because, as noted above, steric hindrance of the reactive site can yield erroneously low reaction efficiencies.[21,64,65] Still, reactions with $TMSN_3$ show that carboxylate ions are produced almost exclusively from aprotic solvents, while proton transfer reactions find a carboxylate structure to be the lowest energy gas-phase conformer or isomer of deprotonated tyrosine

The different deprotonated tyrosine ion structures generated from protic versus aprotic solvents may relate to a different tyrosine neutral structure in the two types of solvents. In aqueous solution, amino acids exist in their zwitterionic form in ~10 000 times greater abundance than their non-zwitterion form. In general, the zwitterionic forms of amino acids dominate in protic solvents, where they are stabilized by strong hydrogen bonding to the solvent.[67] Therefore, in our protic solvent system of $CH_3OH$:$H_2O$:$NH_4OH$, neutral tyrosine is a zwitterion. Consequently, during the ESI process, the site that loses a proton to form deprotonated tyrosine is the ammonium group of the zwitterion. In contrast, for aprotic solvents, there is no consistency with regard to whether a neutral amino acid exists in zwitterionic or non-zwitterionic form. The form relates to both the solvent and the amino acid, and is difficult to predict. In general, the larger the side chain of an amino acid, the less likely it is to exist as a zwitterion in aprotic solvents because steric hindrance will limit solvation.[67,68] Due to the low solubility of tyrosine in most solvents, almost nothing is known about the form of its neutral in nonaqueous solvents. However, tyrosine has one of the largest amino acid side chains, which suggests that its neutral exists as a non-zwitterion in aprotic solvents. Therefore, it is likely that, in an aprotic solvent, the ESI process is deprotonating the most acidic site of the non-zwitterion of tyrosine, which is the carboxylic acid group ($pK_a$ = 6.15 for carboxylate deprotonation and $pK_a$ = 10.37 for phenolate deprotonion[3]).

To test the premise that the neutral form of tyrosine differs in protic and aprotic solvents (and that this might account for different gas-phase ion structures), attempts were made to study the solution-phase structure(s) of tyrosine using FT-IR, FT-Raman, and NMR. Solutions saturated with tyrosine were analyzed in solvent systems ranging from 100% aprotic to 100% protic with 0−5% acid or base additive. Unfortunately, we were not able to obtain any usable data with these spectroscopic techniques because of the low solubility of tyrosine in all solvents tested (including water[69]). The fact that tyrosine can be studied by mass spectrometry in these solvents is testimony to the fact that mass spectrometry can analyze very dilute solutions.

The second, faster reacting tyrosine anion population generated from aprotic solvent is also interesting. Reactions with $TMSN_3$ indicate that the aprotic solvent produces 99% carboxylate ions, but the experimental GA from this second ion population exactly matches the experimental GA relating to the phenoxide ion found in protic solvent. This could mean that the less acidic (more elongated) carboxylate structure is converting to the phenoxide due to interactions with the reference compounds. In particular, AFTP is only ~1 kcal/mol more acidic than deprotonation of tyrosine to generate the unfolded carboxylate. During collisions of AFTP neutrals with tyrosine anions, a proton bound dimer intermediate, $[(Tyr-H)^-\cdot H^+\cdot(AFTP-H)^-]$, could form. This dimer might dissociate with conversion of a tyrosine ion from carboxylate to phenoxide. Such a process would not yield a change in mass and, therefore, would not have been apparent in the mass spectra.

Additional support for a conversion between structures is provided by the ATFP reaction data for tyrosine ions produced from protic solvent. As seen in Table 3, for tyrosine anions produced from protic solvent reacting with ATFP, the measured reaction efficiency is 0.53 ± 0.25 (mean ± standard deviation). The high standard deviation illustrates that this data is much less reproducible than all of the other reaction efficiencies that were measured. For this reaction only, the efficiency varied with pressure and was a relatively poor fit to the sum of two exponentials. This data suggested that the ion population was changing in composition as we were studying it. Thus, data for the reactions of ATFP with deprotonated tyrosine ions produced from both protic and aprotic solvents suggest that a gas-phase conversion between carboxylate and phenoxide ion structures can occur.

**Deprotonated Tyrosine Structure as a Function of Hexapole Accumulation Time.** The ratio of carboxylate to phenoxide ions was studied as a function of accumulation time for ions in the hexapole that immediately follows our ESI source. Previously, Kass and co-workers[9] had attributed the inconsistency between their $TMSN_3$ and PES experiments to different ESI source configurations, with shorter accumulation times (100 ms) favoring a carboxylate structure and longer times (1−5 s) favoring a phenoxide structure. Our mass spectrometer has a hexapole for ion accumulation and its time scale can be easily manipulated, allowing us to study accumulation times similar to those for the two instruments used by Kass in the PES and $TMSN_3$ experiments.

Our proton transfer reactions that bracketed GAs in both protic and aprotic solvent systems used a hexapole accumu-

lation time of 0.6−0.7 s. This time was selected because it generally provided the optimal signal intensity for deprotonated tyrosine. In ESI, ions are produced continually but the FT-ICR mass analyzer requires a pulsed packet of ions. To convert a continuous stream of ions into a pulse, ions leaving the ESI source are trapped in the hexapole where they remain until moved into the FT-ICR cell. During the entire accumulation time, the hexapole can accept new ions. Thus, some ions are trapped in the hexapole for almost the entire accumulation time while other more recently formed ions only spend a few milliseconds in the hexapole.

Because proton transfer reactions with ethyl cyanoacetate can readily distinguish the carboxylate and phenoxide tyrosine structures generated from protic solvent systems, reactions with this reference compound were used to monitor the ion populations as a function of hexapole accumulation time. With an extremely short accumulation time of 1 ms, the faster reacting species (i.e., carboxylate) nearly disappears, resulting in 7% carboxylate ions and 93% phenoxide ions. With an accumulation time of 0.7 s (from the data of Table 1), there is 24% carboxylate and 76% phenoxide. For a very long accumulation time of 5 s, the ratios of the two populations remained at ∼24:76.

The effects of accumulation time for ions produced from various solvents were also studied using $TMSN_3$ reactions to measure the carboxylate and phenoxide abundances. Data obtained for three solvent systems is shown in Figure 4. Figure 4a involves a protic solvent system of 74.5:24.5:1 (v/v/v) $CH_3OH$:$H_2O$:$NH_4OH$. At very short accumulation times, the ion population is 55% phenoxide and 45% carboxylate, but this stabilizes at ∼70% phenoxide and ∼30% carboxylate after ∼0.7 s. Similar effects were observed with other protic solvent systems. Figure 4c shows data obtained with an aprotic solvent of 99:1 (v/v) $CH_3OH$:$H_2O$. At short accumulation times, the ions are almost exclusively carboxylate; at a long time of 5 s, ∼3% of the ions are phenoxide. Figure 4b, involving 98:2 (v/v) $CH_3OH$:$H_2O$, is especially interesting because within less than 1 s of accumulation time the ion ratio goes from ∼55% carboxylate/45% phenoxide to the reverse. This experiment was repeated several times over a period of months, and the result was always the same.

The general trend is that, as the ions spend more time in the hexapole, the relative abundance of phenoxide ions increases and carboxylate ions decreases. This is especially pronounced when the ESI solvent system contains at least 2% of a protic solvent such as $H_2O$ or $CH_3OH$. A possibility is a preferential retention of phenoxide ions or a preferential loss of carboxylate ions, although it is difficult to envision a reason for either of these events to occur. Another possibility is that a conversion between structures is occurring. Presumably, this would be the less stable carboxylate ion (experimental GA of 333.5 kcal/mol) converting to the slightly more stable phenoxide ion (experimental GA of 332.4 kcal/mol), just as these ions appear to convert during the reactions with the reference compound ATFP.

Hexapole ion guides are generally known for collisional cooling of ions, but a slight heating of accumulated ions can occur due to a radial stratification effect. This effect is most pronounced for ions of high charge and high mass-to-charge ratio.[70−72] Deprotonated tyrosine ions are singly charged and of relatively low mass, making addition of energy during the hexapole trapping process less likely. However, very little

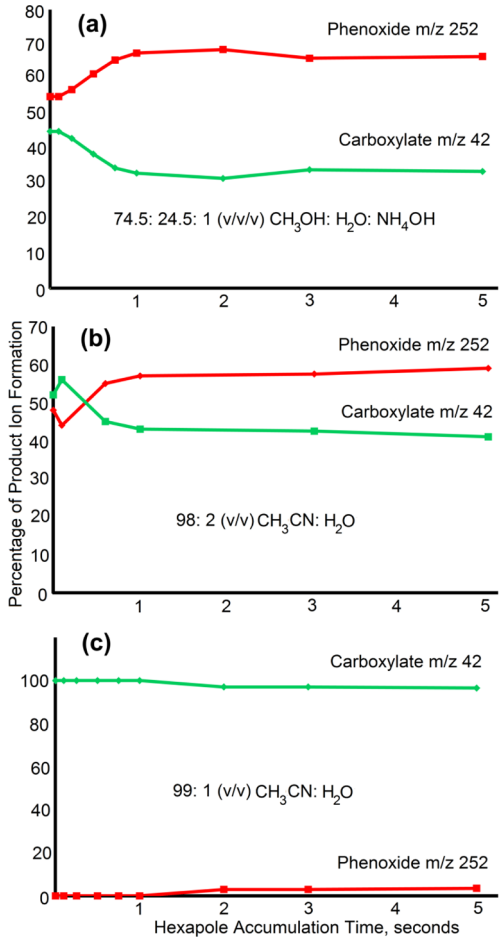


**Figure 4.** Percentage of product ions from the reaction of deprotonated tyrosine with trimethylsilyazide ($TMSN_3$) as a function of time that the ions accumulate in the hexapole. The presence of $m/z$ 252 indicates a phenoxide deprotonated ion structure, while $m/z$ 42 indicates a carboxylate structure. The solvent systems are (a) 74.5:24.5:1 $CH_3OH$:$H_2O$:$NH_4OH$, (b) 98:2 $CH_3CN$:$H_2O$, and (c) 99:1 $CH_3CN$:$H_2O$.

energy would be required to convert between the deprotonated tyrosine isomers and conformers.

If a conversion is occurring, it may be facilitated by solvent interactions with ions in the hexapole. The pressure in the hexapole is in the $10^{-3}$ mbar range, with the primary component being dried air (the ESI drying and nebulizer gas) along with an unknown amount of solvent.[73] The fact that the change in carboxylate/phenoxide ratio is most pronounced in the presence of $H_2O$ supports the involvement of protic solvent (which can hydrogen bond to tyrosine) in an isomerization process. Tian and Kass[8] proposed that there was conversion between the two isomeric structures in the presence of $CH_3OH$. They attributed this effect to a gas-phase relay mechanism[74,75] in which $CH_3OH$ simultaneously coordinates to the deprotonated carboxylic acid and neutral phenol sites, protonating the carboxylate while deprotonating the phenol.

We studied structures for the starting point of the proposed relay mechanism at the DFT level (B3LYP/aug-cc-pVDZ) for the folded and unfolded carboxylate and phenoxide structures with the addition of 2, 3, or 6 waters. Relative energies were calculated for $\Delta G_{gas}$ and $\Delta G_{aq}$ and are given in Table 5. (The optimized structures of the solvated tyrosine anions are shown


dx.doi.org/10.1021/jp510037c | J. Phys. Chem. B 2014, 118, 12630−12643

Table 5. Relative Free Energies in kcal/mol of Solvated Tyrosine

| free energy type[a] | no. of waters | folded carboxylate | unfolded carboxylate | unfolded phenoxide | folded phenoxide |
|---|---|---|---|---|---|
| $\Delta G_{gas}$ | 0 | 1.0 | 0.0 | 1.3 | 8.4 |
| $\Delta\Delta G_{solv}(H_2O)$ | 0 | 1.5 | 0.0 | 6.4 | 10.9 |
| $\Delta\Delta G_{solv}(CH_3OH)$ | 0 | 1.6 | 0.0 | 6.5 | 11.0 |
| $\Delta\Delta G_{solv}(CH_3CN)$ | 0 | 1.4 | 0.0 | 6.5 | 10.9 |
| $\Delta\Delta G_{gas}$ | 2 | 0.0 | 6.5 | 4.3 | 6.0 |
| $\Delta\Delta G_{solv}(H_2O)$ | 2 | 2.5 | 0.0 | 5.8 | 8.5 |
| $\Delta\Delta G_{gas}$ | 3 | 0.0 | 6.2 | 4.0 | 7.1 |
| $\Delta\Delta G_{solv}(H_2O)$ | 3 | 2.5 | 0.0 | 8.8 | 8.7 |
| $\Delta\Delta G_{gas}$ | 6 | 0.0 | 0.5 | 4.4 | 7.8 |
| $\Delta\Delta G_{solv}(H_2O)$ | 6 | 4.0 | 0.0 | 4.4 | 8.1 |

[a] $\Delta\Delta G_{gas}$ = relative free energy in the gas phase. $\Delta\Delta G_{solv}(H_2O)$ = relative free energy in aqueous solution modeled by a self-consistent reaction field. $\Delta\Delta G_{solv}(CH_3OH)$ = relative free energy in methanol solution modeled by a self-consistent reaction field. $\Delta\Delta G_{solv}(CH_3CN)$ = relative free energy in acetonitrile solution modeled by a self-consistent reaction field.

in the Supporting Information.) The Gibbs free energy for deprotonation in aqueous solution ($\Delta G_{aq}$) was calculated from the gas-phase free energy and the aqueous solvation free energy obtained from self-consistent reaction field calculations.[76] The solvation energy was calculated as the sum of the electrostatic energies (polarized solute−solvent) and the nonelectrostatic energies using the COSMO parametrization[77] at the B3LYP/aug-cc-pVDZ level using the gas-phase geometries obtained at this level. Solvents used include $H_2O$, $CH_3OH$, and $CH_3CN$ with respective dielectric constants of 78.39, 32.63, and 36.64.[78] In the gas phase, the folded carboxylate and unfolded phenoxide anions are ∼1 kcal/mol higher in energy than the unfolded carboxylate structure. Without the addition of any explicit waters of solvation, the phenoxide anions are still higher in energy than the carboxylate anions independent of the solvent used. When using a two- or three-water relay mechanism, the folded carboxylate anion is more stable in the gas phase, whereas the unfolded carboxylate is more stable in aqueous solution. In both cases, the phenoxide anions are higher in energy than the carboxylate anions by ∼4−9 kcal/mol. Extra water molecules were added to better solvate the $O^-$ and $COO^-$ sites on the anions. The addition of six waters resulted in the unfolded and folded carboxylate structures having approximately the same energy in the gas phase, whereas in aqueous solution the unfolded carboxylate was still more stable. The unfolded phenoxide structure is more stable with the additional waters and has approximately the same relative energy as the folded carboxylate anion, ∼4 kcal/mol. The stability in solution of the unfolded structure is likely due to an effective larger dipole moment than that for the folded structure. These results show that there is additional chemistry occurring, leading to the experimental observations.

## CONCLUSIONS

Gas-phase deprotonation of the amino acid tyrosine produces three structures: a species deprotonated at the phenolic side chain and two conformers deprotonated at the C-terminal carboxylic acid group. To the best of our knowledge, this is the first time that three distinct structures have been observed when removing a proton from the same small organic precursor molecule by mass spectrometry. The lowest energy, most stable structure is deprotonated at the carboxylic acid group, and G3(MP2) calculations indicate that the structure is highly folded with extensive hydrogen bonding. This structure was only observed experimentally during ESI from aprotic solvents, where tyrosine may exist in a non-zwitterionic form. The second lowest energy structure found experimentally, which is several kcal/mol higher in energy, is deprotonated at the phenol group and is present when the solvent system contains at least 2% of a protic compound. In protic solvent, neutral tyrosine exists as a zwitterion. The third structure is a carboxylate ion, which G3(MP2) calculations indicate to be unfolded. This carboxylate ion is only ∼1.5 kcal/mol higher in energy than the phenolate ion, and the two structures appear to be converting during ion/molecule reactions with some acidic reference compounds and also during ion accumulation in a hexapole. G3(MP2) calculations found that the three structures differ in energy by ∼2.5 kcal/mol, yet all three are readily distinguished experimentally by proton transfer ion/molecule reactions. Experimental conditions, such as solvent and time that ions are accumulated in a hexapole, greatly affect the abundance ratios of the deprotonated tyrosine structures. In contrast, the aromatic amino acid phenylalanine, which has a benzyl side chain, was found experimentally to have one structure when electrosprayed from a protic solvent. This is consistent with the results of G3(MP2) calculations, which indicate that a folded carboxylate structure is only 0.3 kcal/mol more stable than an unfolded carboxylate structure.

## ASSOCIATED CONTENT

### Supporting Information

Complete references for refs 35, 48, and 49. Additional information from the electronic structure calculations including Cartesian *x*, *y*, and *z* coordinates in Å of the lowest energy G3MP2MP2(full)/6-31G(d) and B3LYP/aug-cc-pvdz optimized geometries, total $H_{298}$ and $G_{298}$ energies from Gaussian 09 for all neutrals and anions at the G3(MP2) and B3LYP/aug-cc-pvdz levels, CCSD(T) atomization energies used for the benchmark study of the acidity of formic acid, energy differences of *o*-, *m*-, and *p*-cresol anions at different Gx computational levels, the multiple low energy conformers of the neutral amino acids, solvated tyrosine anions, and higher energy deprotonation sites for the amino acids. This material is available free of charge via the Internet at http://pubs.acs.org.

## AUTHOR INFORMATION

### Present Address

[†](S.S.B.) National Jewish Health, 1400 Jackson Street, Goodman K923, Denver, CO 80206-2761.

### Notes

The authors declare no competing financial interest.

## ■ ACKNOWLEDGMENTS

This research is supported by NSF under CHE-0848470, which is funded by the American Recovery and Reinvestment Act (ARRA) and is jointly sponsored by NSF's Analytical & Surface and Experimental Physical Chemistry sections, and CHE-1308348. S.S.B. thanks the University of Alabama's National Alumni Association for a License Tag Fellowship. M.L.S. and C.E.P. thank the U.S. Department of Education for a Graduate Assistance in Areas of National Need fellowship (DoEd-GAANN grant P200A100190). M.L.S. also thanks the Howard Hughes Medical Institute (HHMI) for a teaching fellowship through the Precollege and Undergraduate Science Education Program. D.A.D. thanks the Robert Ramsay Fund from the University of Alabama for partial support. The assistance of Dr. Ken Belmore and Dr. Russell Timkovich with the NMR experiments is gratefully acknowledged. Some of the CCSD(T) calculations were performed at the Molecular Sciences Computing Facility in the W. R. Wiley Environmental Molecular Sciences Laboratory, a national scientific user facility sponsored by DOE's Office of Biological and Environmental Research and located at Pacific Northwest National Laboratory, operated for the DOE by Battelle.

## ■ REFERENCES

(1) Li, Z.; Matus, M. H.; Velazquez, H. A.; Dixon, D. A.; Cassady, C. J. Gas-Phase Acidities of Aspartic Acid, Glutamic Acid, and their Amino Acid Amides. *Int. J. Mass Spectrom.* **2007**, *265*, 213−223.

(2) Tian, Z.; Pawlow, A.; Poutsma, J. C.; Kass, S. R. Are Carboxyl Groups the Most Acidic Sites in Amino Acids? Gas-Phase Acidity, H/D Exchange Experiments, and Computations on Cysteine and its Conjugate Base. *J. Am. Chem. Soc.* **2007**, *129*, 5403−5407.

(3) Stover, M. L.; Jackson, V.; Matus, M.; Adams, M.; Cassady, C. J.; Dixon, D. A. Fundamental Thermochemical Properties of Amino Acids: Gas-Phase and Aqueous Acidities and Gas-Phase Heats of Formation. *J. Phys. Chem. B* **2012**, *116*, 2905−2916.

(4) DeBlase, A. F.; Kass, S. R.; Johnson, M. A. On the Character of the Cyclic Ionic H-Bond in Cryogenically Cooled Deprotonated Cysteine. *Phys. Chem. Chem. Phys.* **2014**, *16*, 4569−4575.

(5) Oomens, J.; Steill, J. D.; Redlich, B.; Gas-Phase, I. R. Spectroscopy of Deprotonated Amino Acids. *J. Am. Chem. Soc.* **2009**, *131*, 4310−4319.

(6) Bokatzian-Johnson, S. S.; Stover, M. L.; Dixon, D. A.; Cassady, C. J. Gas-Phase Deprotonation of the Peptide Backbone for Tripeptides and their Methyl Esters with Hydrogen and Methyl Side Chains. *J. Phys. Chem. B* **2012**, *116*, 14844−14858.

(7) Gao, J.; Cassady, C. J. Negative Ion Production from Peptides and Proteins by Matrix-Assisted Laser Desorption/ionization Time-of-Flight Mass Spectrometry. *Rapid Commun. Mass Spectrom.* **2008**, *22*, 4066−4072.

(8) Tian, Z.; Kass, S. R. Does Electrospray Ionization Produce Gas-Phase Or Liquid-Phase Structures? *J. Am. Chem. Soc.* **2008**, *130*, 10842−10843.

(9) Tian, Z.; Wang, X. B.; Wang, L. S.; Kass, S. R. Are Carboxyl Groups the most Acidic Sites in Amino Acids? Gas-Phase Acidities, Photoelectron Spectra, and Computations on Tyrosine, p-Hydroxybenzoic Acid, and their Conjugate Bases. *J. Am. Chem. Soc.* **2009**, *131*, 1174−1181.

(10) Bartlett, R. J.; Musial, M. Coupled-Cluster Theory in Quantum Chemistry. *Rev. Mod. Phys.* **2007**, *79*, 291−352.

(11) Kendall, R. A.; Dunning, T. H., Jr.; Harrison, R. J. Electron Affinities of the First-Row Atoms Revisited. Systematic Basis Sets and Wave Functions. *J. Chem. Phys.* **1992**, *96*, 6796−6806.

(12) Li, H.; Lin, Z.; Luo, Y. Gas-Phase IR Spectroscopy of Deprotonated Amino Acids: Global or Local Minima? *Chem. Phys. Lett.* **2014**, *598*, 86−90.

(13) O'Hair, R. A. J.; Bowie, J. H.; Gronert, S. Gas-Phase Acidities of the Alpha-Amino Acids. *Int. J. Mass Spectrom. Ion Processes* **1992**, *117*, 23−36.

(14) Jones, C. M.; Bernier, M.; Carson, E.; Colyer, K. E.; Metz, R.; Pawlow, A.; Wischow, E. D.; Webb, I.; Andriole, E. J.; Poutsma, J. C. Gas-Phase Acidities of the 20 Protein Amino Acids. *Int. J. Mass Spectrom.* **2007**, *267*, 54−62.

(15) Bouchoux, G.; Salpin, J. Y. Re-Evaluated Gas Phase Basicity and Proton Affinity Data from the Thermokinetic Method. *Rapid Commun. Mass Spectrom.* **1999**, *13*, 932−936.

(16) de Koning, L. J.; Nibbering, N. M. M.; van Orden, S. L.; Laukien, F. H. Mass Selection of Ions in a Fourier Transform Ion Cyclotron Resonance Trap using Correlated Harmonic Excitation Fields (CHEF). *Int. J. Mass Spectrom. Ion Processes* **1997**, *165/166*, 209−219.

(17) Bartmess, J. E. In *Negative Ion Energetics Data*; Linstrom, P. J., Ed.; NIST Chemistry WebBook, NIST Standard Reference Database Number 69; National Institute of Standards and Technology: Gaithersburg, MD; http://webbook.nist.gov, (retrieved June 11, 2014).

(18) Zhang, K.; Cassady, C. J.; Chung-Phillips, A. Ab Initio Studies of Neutral and Protonated Triglycines: Comparison of Calculated and Experimental Gas-Phase Basicity. *J. Am. Chem. Soc.* **1994**, *116*, 11512−11521.

(19) Bartmess, J. E.; Georgiadis, R. M. Empirical Methods for Determination of Ionization Gauge Relative Sensitivities for Different Gases. *Vacuum* **1983**, *33*, 149−153.

(20) Miller, K. J. Additivity Methods in Molecular Polarizability. *J. Am. Chem. Soc.* **1990**, *112*, 8533−8542.

(21) Zhang, K.; Zimmerman, D. M.; Chung-Phillips, A.; Cassady, C. J. Experimental and Ab Initio Studies of the Gas-Phase Basicities of Polyglycines. *J. Am. Chem. Soc.* **1993**, *115*, 10812−10822.

(22) Gong, S.; Camara, E.; He, F.; Green, M. K.; Lebrilla, C. B. Chiral Recognition and the Deprotonation Reaction of Gas-Phase Cytochrome c Ions. *Int. J. Mass Spectrom.* **1999**, *185−187*, 401−412.

(23) Jankiewicz, B. J.; Vinueza, N. R.; Kirkpatrick, L. M.; Gallardo, V. A.; Li, G.; Nash, J. J.; Kenttämaa, H. I. Does the 2,6-Didehydropyridinium Cation Exist? *J. Phys. Org. Chem.* **2013**, *26*, 707−714.

(24) He, F.; Marshall, A. G.; Freitas, M. A. Assignment of Gas-Phase Dipeptide Amide Hydrogen Exchange Rate Constants by Site-Specific Substitution: GlyGly. *J. Phys. Chem. B* **2001**, *105*, 2244−2249.

(25) Watkins, M. A.; Nelson, E. D.; Tichy, S. E.; Kenttämaa, H. I. Rearrangement of Phenylcarbene Radical Cation to Dehydrotropylium Cation. *Int. J. Mass Spectrom.* **2006**, *249−250*, 1−7.

(26) Schaaff, T. G.; Stephenson, J. L.; McLuckey, S. A. Gas Phase H/D Exchange Kinetics: DI Versus D2O. *J. Am. Soc. Mass Spectrom.* **2000**, *11*, 167−171.

(27) Gross, D. S.; Schnier, P. D.; Rodriguez-Cruz, S. E.; Fagerquist, C. K.; Williams, E. R. Conformations and Folding of Lysozyme Ions in Vacuo. *Proc. Natl. Acad. Sci. U.S.A.* **1996**, *93*, 3143−3148.

(28) Cassady, C. J.; Carr, S. R. Elucidation of Isomeric Structures for Ubiquitin $[M+12H]^{12+}$ Ions Produced by Electrospray Ionization Mass Spectrometry. *J. Mass Spectrom.* **1996**, *31*, 247−254.

(29) Ewing, N. P.; Cassady, C. J. Effects of Cysteic Acid Groups on the Gas-Phase Reactivity and Dissociation of $[M+4H]^{4+}$ Ions from Insulin Chain B. *J. Am. Soc. Mass Spectrom.* **1999**, *10*, 928−940.

(30) Su, T.; Chesnavich, W. J. Parametrization of the Ion-Polar Molecule Collision Rate-Constant by Trajectory Calculations. *J. Chem. Phys.* **1982**, *76*, 5183−5185.

(31) Su, T. Erratum: Trajectory Calculations of Ion-Polar Molecule Capture Rate Constants at Low Temperatures. *J. Chem. Phys.* **1988**, *89*, 5355−5355.

(32) Bouchoux, G.; Salpin, J. Y.; Leblanc, D. A Relationship Between the Kinetics and Thermochemistry of Proton Transfer Reactions in the Gas Phase. *Int. J. Mass Spectrom. Ion Processes* **1996**, *153*, 37−48.

(33) Bouchoux, G.; Salpin, J. Y. Gas-Phase Basicity of Glycine, Alanine, Proline, Serine, Lysine, Histidine and Some of their Peptides

by the Thermokinetic Method. *Eur. J. Mass Spectrom.* **2003**, *9*, 391−402.
(34) Bouchoux, G.; Buisson, D.; Bourcier, S.; Sablier, M. Application of the Kinetic Method to Bifunctional Bases ESI Tandem Quadrupole Experiments. *Int. J. Mass Spectrom.* **2003**, *228*, 1035−1054.
(35) Frisch, M. J.; Trucks, G. W.; Schlegel, H. B.; Scuseria, G. E.; Robb, M. A.; Cheeseman, J. R.; Scalmani, G.; Barone, V.; Mennucci, B.; Petersson, G. A.; et al. *Gaussian 09*, revision B.0.; Gaussian, Inc.: Wallington, CT, 2010.
(36) Becke, A. D. Density-Functional Thermochemistry. III. The Role of Exact Exchange. *J. Chem. Phys.* **1993**, *98*, 5648−5652.
(37) Parr, R. G.; Yang, W. In *Density Functional Theory of Atoms and Molecules*; Oxford University Press: New York, 1989.
(38) Godbout, N.; Salahub, D. R.; Andzelm, J.; Wimmer, E. Optimization of Gaussian-Type Basis Sets for Local Spin Density Functional Calculations. Part I. Boron through Neon, Optimization Technique and Validation. *Can. J. Chem.* **1992**, *70*, 560−571.
(39) Gutowski, K. E.; Dixon, D. A. Ab Initio Prediction of the Gas- and Solution-Phase Acidities of Strong Bronsted Acids: The Calculation of pKa Values Less than −10. *J. Phys. Chem. A* **2006**, *110*, 12044−12054.
(40) Curtiss, L. A.; Redfern, P. C.; Raghavachari, K.; Rassolov, V.; Pople, J. A. Gaussian-3 Theory using Reduced Moller-Plesset Order. *J. Chem. Phys.* **1999**, *110*, 4703−4709.
(41) Dixon, D. A.; Feller, D.; Peterson, K. A. In *A Practical Guide to Reliable First Principles Computational Thermochemistry Predictions Across the Periodic Table*; Wheeler, R. A., Section Ed., Tschumper, G. S., Eds.; Annual Reports in Computational Chemistry; Elsevier: Amsterdam, The Netherlands, 2012; Vol. *8*, pp 1−28.
(42) Feller, D.; Peterson, K. A.; Dixon, D. A. Further Benchmarks of a Composite, Convergent, Statistically Calibrated Coupled-Cluster-Based Approach for Thermochemical and Spectroscopic Studies. *Mol. Phys.* **2012**, *110*, 2381−2399.
(43) Peterson, K. A.; Feller, D.; Dixon, D. A. Chemical Accuracy in Ab Initio Thermochemistry and Spectroscopy: Current Strategies and Future Challenges. *Theor. Chem. Acc.* **2012**, *131*, 1−20.
(44) Feller, D.; Peterson, K. A.; Dixon, D. A. A Survey of Factors Contributing to Accurate Theoretical Predictions of Atomization Energies and Molecular Structures. *J. Chem. Phys.* **2008**, *129*, 204105/1−204105/32.
(45) Feller, D.; Dixon, D. A. Extended Benchmark Studies of Coupled Cluster Theory through Triple Excitations. *J. Chem. Phys.* **2001**, *115*, 3484−3496.
(46) McQuarrie, D. A. *Statistical Mechanics*; Harper & Row: New York, 1976.
(47) Muftakhov, M. V.; Vasil'ev, Y. V.; Mazunov, V. A. Determination of Electron Affinity of Carbonyl Radicals by Means of Negative Ion Mass Spectrometry. *Rapid Commun. Mass Spectrom.* **1999**, *13*, 1104−1108.
(48) Knowles, P. J.; Manby, F. R.; Schütz, M.; Celani, P.; Knizia, G.; Korona, T.; Lindh, R.; Mitrushenkov, A.; Rauhut, G.; Adler, T. B.; et al. *MOLPRO, version 2010.1, A Package of Ab Initio Programs*; University College Cardiff Consultants Limited: Cardiff, Wales, UK, 2010; http://www.molpro.net/.
(49) Valiev, M.; Bylaska, E. J.; Govind, N.; Kowalski, K.; Straatsma, T. P.; Van Dam, H. J. J.; Wang, D.; Nieplocha, J.; Apra, E.; Windus, T. L.; et al. NWChem: A Comprehensive and Scalable Open-Source Solution for Large Scale Molecular Simulations. *Comput. Phys. Commun.* **2010**, *181*, 1477−1489.
(50) Curtiss, L. A.; Raghavachari, K. Gaussian-3 (G3) Theory for Molecules Containing First and Second-Row Atoms. *J. Chem. Phys.* **1998**, *109*, 7764−7776.
(51) Baboul, A. G.; Curtiss, L. A.; Redfern, P. C.; Raghavachari, K. Gaussian-3 Theory using Density Functional Geometries and Zero-Point Energies. *J. Chem. Phys.* **1999**, *110*, 7650−7657.
(52) Curtiss, L. A.; Redfern, P. C.; Raghavachari, K. Gaussian-4 Theory. *J. Chem. Phys.* **2007**, *126*, 084108/1−084108/12.
(53) Curtiss, L. A.; Redfern, P. C.; Raghavachari, K. Gaussian-4 Theory using Reduced Order Perturbation Theory. *J. Chem. Phys.* **2007**, *127*, 124105/1−124105/8.
(54) Cumming, J. B.; Kebarle, P. Summary of Gas Phas Acidity Measurements Involving Acids AH. Entropy Changes in Proton Transfer Reactions Involving Negative Ions. Bond Dissociation Energies D(A-H) and Electron Affiniites EA(A). *Can. J. Chem.* **1978**, *56*, 1−9.
(55) Angel, L. A.; Ervin, K. M.; Gas-Phase Acidities; Bond, O.-H. Dissociation Enthalpies of Phenol, 3-Methylphenol, 2,4,6-Trimethylphenol, and Ethanoic Acid. *J. Phys. Chem. A* **2006**, *110*, 10392−10403.
(56) Harrison, A. G.; Tu, Y. Site of Protonation of N-Alkylanilines. *Int. J. Mass Spectrom.* **2000**, *195/196*, 33−43.
(57) Harrison, A. G. *Chemical Ionization Mass Spectrometry*; CRC Press: Boca Raton, FL, 1992.
(58) Lau, Y. K.; Kebarle, P. Substituent Effects on the Intrinsic Basicity of Benzene: Proton Affinities of Substituted Benzenes. *J. Am. Chem. Soc.* **1976**, *98*, 7452−7453.
(59) McLuckey, S. A.; Cameron, D.; Cooks, R. G. Proton Affinities from Dissociations of Proton-Bound Dimers. *J. Am. Chem. Soc.* **1981**, *103*, 1313−1317.
(60) Cheng, X.; Wu, Z.; Fenselau, C. Collision Energy Dependence of Proton-Bound Dimer Dissociation: Entropy Effects, Proton Affinities, and Intramolecular Hydrogen Bonding in Protonated Peptides. *J. Am. Chem. Soc.* **1993**, *115*, 4844−4848.
(61) Haupert, L. J.; Poutsma, J. C.; Wenthold, P. G. The Curtin-Hammett Principle in Mass Spectrometry. *Acc. Chem. Res.* **2009**, *42*, 1480−1488.
(62) Fournier, F.; Afonso, C.; Fagin, A. E.; Gronert, S.; Tabet, J. C. Can Cluster Structure Affect Kinetic Method Measurements? the Curious Case of Glutamic Acid's Gas-Phase Acidity. *J. Am. Soc. Mass Spectrom.* **2008**, *19*, 1887−1896.
(63) Jia, B.; Angel, L. A.; Ervin, K. M. Threshold Collision-Induced Dissociation of Hydrogen-Bonded Dimers of Carboxylic Acids. *J. Phys. Chem. A* **2008**, *112*, 1773−1782.
(64) Buker, H.-H.; Grutzmacher, H.-F. A Fourier Transform-Ion Cyclotron Resonance Study of Steric Effects on Proton Transfer Reactions of Polyalkyl Benzenes. *Int. J. Mass Spectrom. Ion Processes* **1991**, *109*, 95−104.
(65) Attina, M.; Cacace, F. Concerning Sterical Hindrance to Deprotonation of Gaseous Polyalkylbenzenium Ions. *Int. J. Mass Spectrom. Ion Processes* **1992**, *120*, R1−R4.
(66) Schröder, D.; Budesinsky, M.; Roithova, J. Deprotonation of p-Hydroxybenzoic Acid: Does Electrospray Ionization Sample Solution or Gas-Phase Structures? *J. Am. Chem. Soc.* **2012**, *134*, 15897−15905.
(67) Hughes, D. L.; Bergan, J. J.; Grabowski, E. J. J. Amino Acid Chemistry in Dipolar Aprotic Solvents: Dissociation Constants and Ambident Reactivity. *J. Org. Chem.* **1986**, *51*, 2579−2585.
(68) Cheung, E. T. Substituent Effects on the Tautomerization of Amino Acids. MS Thesis, Texas Tech University, Lubbock, TX, 1995.
(69) Lide, D. R., Ed. *CRC Handbook of Chemistry and Physics*; CRC Press: Cleveland, OH, 1992−1993.
(70) Tolmachev, A. V.; Udseth, H. R.; Smith, R. D. Radial Stratification of Ions as a Function of Mass to Charge Ratio in Collisional Cooling Radio Frequency Multipoles used as Ion Guides or Ion Traps. *Rapid Commun. Mass Spectrom.* **2000**, *14*, 1907−1913.
(71) McDonnell, L. A.; Giannakopulos, A. E.; Derrick, P. J.; Tsybin, Y. O.; Hakansson, P. A. Theoretical Investigation of the Kinetic Energy of Ions Trapped in a Radio-Frequency Hexapole Ion Trap. *Eur. J. Mass Spectrom.* **2002**, *8*, 181−189.
(72) Tolmachev, A. V.; Udseth, H. R.; Smith, R. D. Modeling the Ion Density Distribution in Collisional Cooling RF Multipole Ion Guides. *Int. J. Mass Spectrom.* **2003**, *222*, 155−174.
(73) Easterling, M. L., Bruker Daltonics FT-ICR Product Manager. Private correspondence, March 28, 2012.
(74) Campbell, S.; Rodgers, M.; Marzluff, E.; Beauchamp, J. Deuterium Exchange Reactions as a Probe of Biomolecule Structure. Fundamental Studies of Gas Phase H/D Exchange Reactions of

Protonated Glycine Oligomers with $D_2O$, $CD_3OD$, $CD_3CO_2D$, and $ND_3$. *J. Am. Chem. Soc.* **1995**, *117*, 12840−12854.
(75) Gard, E.; Green, M. K.; Bregar, J.; Lebrilla, C. B. Gas-Phase Hydrogen/Deuterium Exchange as a Molecular Probe for the Interaction of Methanol and Protonated Peptides. *J. Am. Soc. Mass Spectrom.* **1994**, *5*, 623−631.
(76) Tomasi, J.; Mennucci, B.; Cammi, R. Quantum Mechanical Continuum Solvation Models. *Chem. Rev.* **2005**, *105*, 2999−3094.
(77) Klamt, A.; Schüürmann, G. COSMO: A New Approach to Dielectric Screening in Solvents with Explicit Expressions for the Screening Energy and its Gradient. *J. Chem. Soc., Perkin Trans. 2* **1993**, 799−805.
(78) Cammi, R.; Mennucci, B.; Tomasi, J. In *Computational Modelling of the Solvent Effects on Molecular Properties: An Overview of the Polarizable Continuum Model (PCM) Approach*; Leszczynski, J., Ed.; Computational Chemistry: Reviews of Current Trends; World Scientific: Singapore, 2003; Vol. *8*, pp 1−79.
(79) Fujio, M.; McIver, R. T.; Taft, R. W. Effects of the Acidities of Phenols from Specific Substituent-Solvent Interactions. Inherent Substituent Parameters from Gas-Phase Acidities. *J. Am. Chem. Soc.* **1981**, *103*, 4017−4029.
(80) Caldwell, G.; Renneboog, R.; Kebarle, P. Gas-Phase Acidities of Aliphatic Carboxylic Acids, Based on Measurements of Proton Transfer Equilibria. *Can. J. Chem.* **1989**, *67*, 611−618.
(81) Kim, E. H.; Bradforth, S. E.; Arnold, D. W.; Metz, R. B.; Neumark, D. M. Study of $HCO_2$ and $DCO_2$ by Negative Ion Photoelectron Spectroscopy. *J. Chem. Phys.* **1995**, *103*, 7801−7814.
(82) Taft, R. W.; Topsom, R. D. The Nature and Analysis of Substitutent Electronic Effects. *Prog. Phys. Org. Chem.* **1987**, *16*, 1−84.
(83) Jinfeng, C.; Topsom, R. D.; Headley, A. D.; Koppel, I.; Mishima, M.; Taft, R. W.; Veji, S. Acidities of Substituted Acetic Acids. *J. Mol. Struct.: THEOCHEM* **1988**, *168*, 141−146.
(84) Norrman, K.; McMahon, T. B. Intramolecular Solvation of Carboxylate Anions in the Gas Phase. *J. Phys. Chem. A* **1999**, *103*, 7008−7016.
(85) Richardson, J. H.; Stephenson, L. M.; Brauman, J. I. Photodetachment of Electrons from Phenoxides and Thiophenoxide. *J. Am. Chem. Soc.* **1975**, *97*, 2967−2970.
(86) Bartmess, J. E.; Scott, J. A.; McIver, R. T. Scale of Acidities in the Gas-Phase from Methanol to Phenol. *J. Am. Chem. Soc.* **1979**, *101*, 6046−6056.
(87) Gunion, R. F.; Gilles, M. K.; Polak, M. L.; Lineberger, W. C. Ultraviolet Photoelectron Spectroscopy of the Phenide, Benzyl and Phenoxide Anions, with Ab Initio Calculations. *Int. J. Mass Spectrom. Ion Processes* **1992**, *117*, 601−620.
(88) DeTuri, V. F.; Ervin, K. M. Proton Transfer between $Cl^-$ and $C_6H_5OH$. O-H Bond Energy of Phenol. *Int. J. Mass Spectrom. Ion Processes* **1998**, *175*, 123−132.
(89) Angel, L. A.; Ervin, K. M. Competitive Threshold Collision-Induced Dissociation: Gas-Phase Acidity and O-H Bond Dissociation Enthalpy of Phenol. *J. Phys. Chem. A* **2004**, *108*, 8346−8352.
(90) McMahon, T. B.; Kebarle, P. Intrinsic Acidities of Substituted Phenols and Benzoic Acids Determined by Gas-Phase Proton-Transfer Equilibria. *J. Am. Chem. Soc.* **1977**, *99*, 2222−2230.